Extreme Mechanics Letters 31 (2019) 100534

Contents lists available at ScienceDirect

Extreme Mechanics Letters

journal homepage: www.elsevier.com/locate/eml

Nanoscale silicon-based actuators with extremely large actuation strain and extremely low driving voltage

Jiamei Guo, Zheng Jia *

Center for X-Mechanics, Key Laboratory of Soft Machines and Smart Devices of Zhejiang Province, Department of Engineering Mechanics, Zhejiang University, Hangzhou, 310027, China

ARTICLE INFO

Article history:
Received 21 June 2019
Received in revised form 25 July 2019
Accepted 30 July 2019
Available online 1 August 2019

Keywords:
Actuation
Lithiation
Silicon
Stress
Strain of actuation

ABSTRACT

The coupling between lithiation reaction of silicon and the considerable volume change has been widely recognized as an adverse effect which hinders the practical application of silicon-based lithium-ion batteries. Here we theoretically demonstrate a novel class of nanoscale electrochemically-driven silicon actuators, in virtue of the "unfavorable" gigantic volume expansion engendered by lithiation. Two representative design prototypes are reported, namely, a nano-sized flat-film silicon actuator and a nanowire silicon actuator. Our thermodynamic analysis establishes the operation condition of the actuators by identifying the electrochemical driving force and mechanical resistance due to lithiation-induced stress. We show that the nano-actuator exhibits an extremely low driving voltage about 1 V and an extremely high strain of actuation up to 300%, which goes far beyond the features of most common actuator materials. Given a mechanical load, the flat-film silicon actuator features a constant actuation strain and the nanowire actuator can provide tunable actuation strain. The results from the study offer quantitative guidance to the design of the novel silicon-based nano-actuators.

Silicon has been highlighted as a promising alternative to conventional graphite, owing to its superior specific capacity which is one order of magnitude higher than that of graphite anodes. The high theoretical capacity arises from the ability to host substantially more lithium than graphite. Nevertheless, the insertion of a large number of lithium atoms leads to considerable volume expansion (about 300%) of the silicon, which causes structural destruction of the electrode and severe capacity fading, thereby hindering the practical application of silicon anode in commercial batteries [1,2]. In order to put silicon into use as a practical anode, tremendous efforts have been devoted to alleviating the mechanical failure of silicon anodes induced by the excessive volume expansion, typically by nano-structuring [2], nano-compositing [3,4], designing microporous structures [5,6], or exploiting novel binders to hold silicon particles together [7]. Now that mechanical degradation of Si due to the huge volumetric change has been mitigated to varying degrees of success with the aforementioned strategies.

Although a significant amount of research has been performed with the goal of addressing the adverse effect of lithiation-induced expansion, few efforts have been made to instead harness the gigantic lithiation-induced strain to provide useful functions. For its first time, Lang et al. demonstrated a macroscale actuator based on a LiFePO4/Si full cell which can drive a large mechanical load with an output strain about 1% [8]. Macroscopic actuators based on Li-reactive materials beyond silicon, such as germanium, were also reported [9]. In addition to the lithiation-enabled actuator, researchers also developed generators based on electrode materials by taking advantage of the stress-regulated lithiation kinetics [10,11]. Kim et al. developed a new class of energy-harvesting device comprised of two partially lithiated silicon films sandwiching an electrolyte [11]. Through stress–voltage coupling, the asymmetric stress state engendered by bending gives rise to a chemical potential difference which drives the charge carriers to shuttle between the two electrodes, thereby converting mechanical energy into electrical energy [12].

The functionality of the abovementioned actuator and generator arises from the lithiation-induced strain and the stress-mediated lithiation, respectively. Herein, we theoretically demonstrate a new type of nanoscale actuator based on the unique two-phase lithiation mechanism of nano-sized silicon [13–16], by harnessing the intimate coupling between lithiation and mechanics. Two prototypes are presented, i.e., a flat-film silicon actuator (Fig. 1a) and a nanowire silicon actuator (Fig. 1c). Our analysis predicts that driven by an extremely low input voltage below 1 V, the nanoscale actuators based on lithiation of silicon exhibit an extremely high actuation strain up to 300% and an extremely large actuation stress beyond 1 GPa, which is superior to common electroactive actuator materials. Moreover, the fully coupled lithiation kinetics and mechanical stress endow the

* Corresponding author.
E-mail address: zheng.jia@zju.edu.cn (Z. Jia).

https://doi.org/10.1016/j.eml.2019.100534
2352-4316/

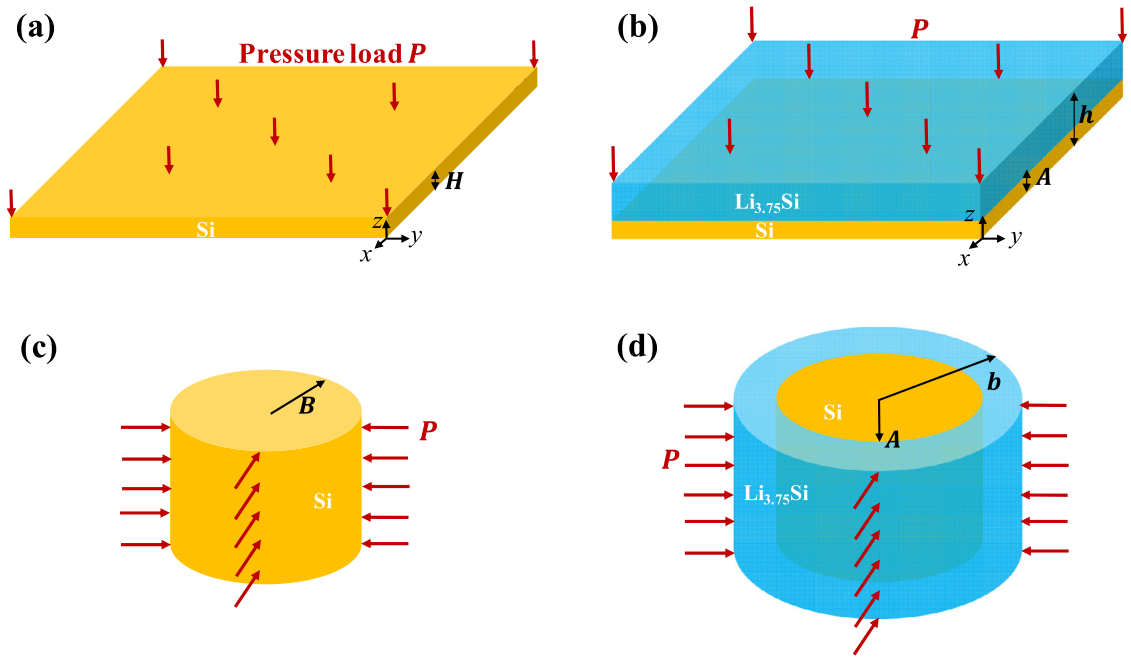

Fig. 1. Schematics of the conceptual lithiated-silicon-based actuator. (a) The initial flat-film silicon actuator of thickness H. A uniform pressure P is imposed to the top surface of the film to represent the mechanical load to be actuated. (b) The working principle of the nanoscale flat-film actuator. Upon lithiation, lithium ions are inserted into the film through its top surface, the silicon film becomes a double-layer structure consisting of a top lithiated layer (blue) and a bottom pristine layer (yellow) which are separated by an interface (namely, the reaction front) at $z = A$. The lithiated phase thickens continuously as the reaction front moves downwards, thereby lifting the mechanical loads. (c) The initial configuration of the nanowire silicon actuator of radius B. (d) The working principle of the nanowire actuator. Lithium ions migrate into the nanowire through its lateral surface and the reaction front of $r = A$ moves towards the center of the nanowire, which causes the shrinkage of the remaining silicon core (yellow) and the expansion of the lithiated shell (blue), thus pushing out the mechanical loads. The current outer radius of the actuator is given by b. (For interpretation of the references to color in this figure legend, the reader is referred to the web version of this article.)

nanowire actuator with tunable actuation strain, which has not been achieved by the macroscale actuators based on Li–Si alloy.

To illustrate essential ideas, we sketch the schematics of the two types of nanoscale actuators in Fig. 1, namely, a flat silicon film (Fig. 1a and c) and a silicon nanowire (Fig. 1b and d) subjected to lithiation reaction. A uniform pressure P is applied to the top surface of the film and the lateral surface of the nanowire, respectively, to model the dead loads that to be displaced by the nano-actuators. We take the flat-silicon film (Fig. 1a) as an example to elucidate the working principle of the silicon-based actuators. It is important to recognize that the actuator design presented in the current study is based on the lithiation of pristine silicon, a process intrinsically different than the lithiation of post-lithiated alloys (namely, silicon or germanium that already undergoes various degrees of lithiation and delithiation). Consequently, the actuation mechanism of the nanoscale actuator proposed here is governed by the reaction kinetics between lithium and fresh silicon, instead of the diffusion kinetics of lithium in the lithiated phase. Under the operation condition, lithium ions enter the flat silicon film through its top surface, thus the film becomes a bilayer structure composed of a top lithiated layer ($Li_{3.75}Si$, blue in Fig. 1) and a bottom pristine silicon layer (yellow) which are separated by a phase interface, as illustrated in Fig. 1b. Lithium atoms continuously diffuse to the interface and react with fresh silicon, transforming the silicon phase to the lithiated silicon phase and generating significant volume expansion. As a consequence, the phase interface moves downwards and the lithiated layer thickens drastically, thereby driving large actuation of the mechanical loads. The actuation goes on until the lithiation reaction halts. (To be consistent with the nomenclature adopted in the reference [17], we will refer to the phase interface as the reaction front hereafter since the lithiation reaction occurs on the interface.)

We next quantitatively identify the operation condition of the silicon-based nano-actuators. As analyzed above, the "engine" of the actuator is the lithiation reaction taking place at the reaction front which converts lithium ions (namely, the "fuel" for the engine), electrons, and silicon atoms into the $Li_{3.75}Si$ phase and simultaneously generates actuation strain. The lithiation reaction can be described by the chemical reaction equation that

$$\mathrm{Li}^+ + \mathrm{e}^- + \frac{1}{3.75}\mathrm{Si} = \frac{1}{3.75}\mathrm{Li}_{3.75}\mathrm{Si} \tag{1}$$

The change in free energy associated with the reaction (i.e., the free energy of the products minus that of the reactants) can be identified as $\Delta G = \Delta G_{chem} + \Delta G_{elec} + \Delta G_{mech}$. ΔG_{chem} denotes the change in free energy associated with the chemical reaction when both applied voltage and stress vanish. $\Delta G_{elec} = -e\Phi$ is the energy change due to the work done by the voltage, where Φ is the voltage applied to the actuator (i.e., the bias voltage between the silicon and the lithium source) and e the elementary charge. It should be pointed out that experimental studies have evidenced that the value of applied voltage Φ remains a constant under both potentiostatic condition and galvanostatic condition since the lithiation of nano-sized silicon is a reaction limited process [18]. ΔG_{mech} represents the contribution of lithiation-induced stress to the free energy change.

According to the definition of ΔG, a negative ΔG triggers the reaction, which starts the "engine" of the actuator and drives it to lift loads, while a non-negative ΔG arrests the reaction and shut down the "engine" of the actuator. That is to say, the actuator functions when $\Delta G_{mech} < e\phi - \Delta G_{chem}$, but the actuator loses power if $\Delta G_{mech} \geq e\phi - \Delta G_{chem}$. The value of $e\Phi$ is dictated by the applied voltage Φ and always takes a positive value. It has been reported that ΔG_{chem} is intrinsically negative, for instance, $\Delta G_{chem} = -0.18$ eV for $Li_{2.1}Si$ [19]. It follows that the term of $e\phi - \Delta G_{chem}$ remains a constant once an external voltage is applied.

Consequently, whether the actuator works or stalls hinges upon the value of ΔG_{mech}. We evaluate ΔG_{mech} as follows: strain energy density stored on the reaction front (i.e., $-\sigma_m^{Li_{3.75}Si}\Omega^{Li_{3.75}Si}$) minus that of the unlithiated silicon phase (i.e., $-\sigma_m^{Si}\Omega^{Si}$), so that

$$\Delta G_{mech} = \frac{1}{3.75}[\sigma_m^{Si}\Omega^{Si} - \sigma_m^{Li_{3.75}Si}\Omega^{Li_{3.75}Si}] \tag{2}$$

where σ_m^{Si} and $\sigma_m^{Li_{3.75}Si}$ denote the mean stress ($\sigma_m = \frac{\sigma_x+\sigma_y+\sigma_z}{3}$) in the unlithiated silicon phase and the mean stress in the fully lithiated phase on the reaction front, respectively. Ω^{Si} and $\Omega^{Li_{3.75}Si}$ represent the volume per unit of Si and $Li_{3.75}Si$, respectively. According to Eq. (2), to determine the value of ΔG_{mech}, lithiation-induced stress profile in the Li–Si alloy actuator needs to be obtained.

We first analyze the stress field developed in the flat silicon film as illustrated in Fig. 1a, with its top surface subjected to the lithium insertion and a pressure P exerted by the load. The pristine film, with thickness H, is taken as the reference configuration. During lithiation, the film becomes a double-layer structure which is comprised of a top Li-rich layer and an underlying Li-free layer, with the position of the interface being $z = A$, and the current thickness of the film being h. The Li–Si alloy film functions as an actuator by lifting the load via continuous thickening (Apparently, $h > H$) due to lithiation. To focus on the main ideas, we neglect the elastic deformation of the lithiated silicon and model it as a rigid-plastic material. Consequently, the thickening of the lithiated silicon is entirely a result of lithiation-induced volume expansion. In the present work, we are modeling a flat-film actuator lifting loads with the lateral expansion of the film mechanically constrained. That is, the in-plane expansion (along x and y directions) of the film is strongly restricted during lithiation and thus the large volumetric expansion associated with the lithiation is accommodated by elongating the lithiated silicon in the z direction. Consider a material element on the lithiation front, the total stretches are given by $\lambda_z = \beta$ and $\lambda_x = \lambda_y = 1$, where $\beta = \Omega^{Li_\eta Si}/\Omega^{Si}$ ($0 \le \eta \le 3.75$) represents the volume expansion ratio due to lithiation which increases from 1 (pristine silicon, $\eta = 0$) to 4 (fully lithiated silicon, $\eta = 3.75$) at the reaction front. Then the plastic stretches at the reaction front are obtained as follows: $\lambda_z^p = \lambda_z\beta^{-\frac{1}{3}} = \beta^{\frac{2}{3}}$ and $\lambda_x^p = \lambda_y^p = \beta^{-\frac{1}{3}}$. Given the correlation between the stretch ratio and the true strain, the increment of true strains can be expressed as $\delta\varepsilon_z^p = \frac{2}{3}\frac{\delta\beta}{\beta}$ and $\delta\varepsilon_x^p = \delta\varepsilon_y^p = -\frac{1}{3}\frac{\delta\beta}{\beta}$, with the equivalent plastic strain being $\delta\varepsilon_{eq}^p = \frac{2}{3}\frac{\delta\beta}{\beta}$. Let σ_Y be the yielding stress of lithiated silicon, then the J_2 flow rule gives the deviatoric stress components that $s_z = \frac{2}{3}\frac{\sigma_Y}{\delta\varepsilon_{eq}^p}\delta\varepsilon_z^p = \frac{2}{3}\sigma_Y$ and $s_x = s_y = -\frac{1}{3}\sigma_Y$. The silicon film is subjected to a uniform pressure P on its top surface, such that the resulting stress in the direction normal to the film is given by $\sigma_z = -P$. The mean stress σ_m on the reaction front is given by $\sigma_z - s_z = -P - \frac{2}{3}\sigma_Y$. Consequently, the stress profile on the lithiation front ($z = A$) can be written as

$$\sigma_x = \sigma_y = -\sigma_Y - P, \tag{3}$$

$$\sigma_z = -P, \tag{4}$$

The unlithiated pristine silicon film lies underneath the fully lithiated part of the actuator and thus is characterized by $0 < z < A$. Taking pristine silicon as a linear elastic material, we obtain the stress field in the unlithiated silicon phase by solving a plane-strain problem (i.e., $\varepsilon_x = \varepsilon_y = 0$),

$$\sigma_x = \sigma_y = -\frac{\nu}{1-\nu}P, \tag{5}$$

$$\sigma_z = -P, \tag{6}$$

where ν is the Poisson's ratio of the pristine silicon phase.

Eqs. (3)–(6) indicate that the mean stress at the reaction front and in the remaining pristine silicon phase can be expressed as $\sigma_m^{Li_{3.75}Si} = -P - \frac{2}{3}\sigma_Y$ and $\sigma_m^{Si} = -\frac{1+\nu}{3(1-\nu)}P$, respectively. Inserting these expressions into Eq. (2), one has

$$\Delta G_{mech} = \frac{\Omega^{Si}}{3.75}\left[\left(\beta_{max} - \frac{1+\nu}{3(1-\nu)}\right)P + \frac{2}{3}\sigma_Y\beta_{max}\right] \tag{7}$$

where β_{max} is the volume change ratio from the pristine silicon phase to the fully lithiated silicon phase, which is defined by $\beta_{max} = \frac{\Omega^{Li_{3.75}Si}}{\Omega^{Si}} = 4$, embodying the effect of lithiation on deformation.

The evolution of ΔG_{mech} as the lithiation proceeds is plotted in Fig. 2a, where the horizontal axis is the normalized position of the reaction front A/h. To examine the effect of the loads that to be lifted by the actuator on the value of ΔG_{mech}, the applied pressure P is taken to be 0 GPa (no load), 5 GPa, and 8 GPa, respectively. In this work, we take $\Omega^{Si} = 2 \times 10^{-29}$ m^3 [20], $\beta_{max} = 4$ [20], $\sigma_Y = 1.5$ GPa [20] and $\nu = 0.24$ [20]. For a given load, namely, a constant applied pressure P, the value of ΔG_{mech} is independent of the position of the reaction front A/h and remains a constant as the reaction advances. In addition, we find that ΔG_{mech} is always positive and increases with increasing P. For example, ΔG_{mech} takes a value of 0.13 eV (the black line), 0.71 eV (the red line), and 1.06 eV (the blue line) for $P = 0$ GPa, 5 GPa, and 8 GPa, respectively. Recall that the condition under which the Li–Si alloy actuator functions is given by $\Delta G_{mech} < e\phi - \Delta G_{chem}$. The left-hand side of the equation (namely, ΔG_{mech}) can be regarded as a parameter that measures the mechanical resistance due to the load, and the term on the right (i.e., $e\phi - \Delta G_{chem}$) denotes the electrochemical driving force for the actuator, so that the nano-actuator functions only when the driving force overcomes the mechanical resistance. In Fig. 2a, we sketch the driving force term $e\phi - \Delta G_{chem}$ with the applied voltage being $\phi = 0.6$ eV as the dashed line. The results show that the magnitude of $e\phi - \Delta G_{chem}$ exceeds ΔG_{mech} for $P = 0$ GPa and 5 GPa, but becomes smaller than ΔG_{mech} when P is increased to 8 GPa. That is, the actuator powered by an external voltage of $\phi = 0.6$ eV is capable of driving loads of $P = 0$ GPa and 5 GPa, but fails in actuating comparatively large load of $P = 8$ GPa, because the heavy load can readily generate large enough mechanical resistance (ΔG_{mech}) to counter-balance the driving force ($e\phi - \Delta G_{chem}$), thereby stalling the actuator. It is worthwhile to note that, in this numerical example, driven by a voltage as low as 0.6 V, the flat-film actuator can move an extremely large load of 5 GPa, demonstrating the strong power of the nano-sized silicon actuator. The working principle of the nano-actuator can also be understood in terms of the overpotential, As shown in Fig. 2a, the load of $P = 8$ GPa exerts a stress-induced overpotential of 1.06 V to the nano-actuator, counterbalancing the electrochemical driving force equivalent to 0.78 V and stalling the actuator. In contrast, the load of $P = 5$ GPa imposes an overpotential of 0.71 V which is inadequate to offset the electrochemical driving force, such that the silicon film can lift the load of $P = 5$ GPa.

One important indicator of the function of actuators is the strain of actuation. For the flat-film silicon actuator, the strain of actuation ε_a is related to the final thickness of the film $\tilde{h}$ after the actuation stalls and the initial film thickness H, by $\varepsilon_a = \frac{\tilde{h}}{H} - 1$. As evident in Fig. 3a, for small loads P, the mechanical resistance curve (black and red lines) is lower than the driving force curve (the dashed line) for all range of A/h, indicating that the actuation continues until the entire silicon film is lithiated. Note that h can be written in terms of H and A by $h = A + \beta_{max}(H - A)$. Upon complete lithiation of the film, $A = 0$ and $\tilde{h} = \beta_{max}H$ so that the actuation strain is given by $\varepsilon_a = \beta_{max} - 1 = 300\%$. Therefore, the strain of actuation achievable by the flat-film silicon actuator is 300% for small loads. Fig. 2a also demonstrates that when the

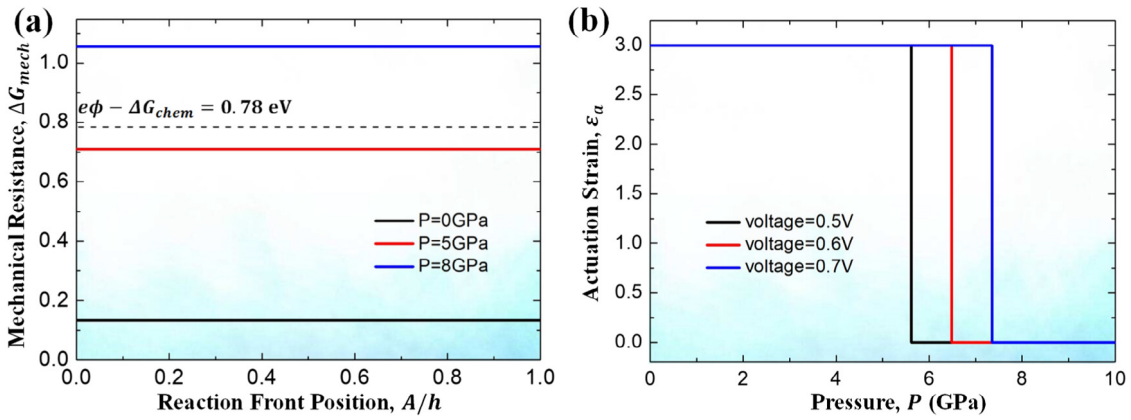

Fig. 2. (a) The mechanical resistance due to lithiation-induced stress as a function of the reaction front position A/h. The effect of different mechanical loads is investigated by varying P. (b) The output actuation strain with different mechanical loads P and applied voltages Φ. (For interpretation of the references to color in this figure legend, the reader is referred to the web version of this article.)

applied pressure exceeds a critical value, the magnitude of the resistance ΔG_{mech} (for example, the blue line corresponding to $P = 8$ GPa) becomes larger than the driving force $e\phi - \Delta G_{chem}$. As a consequence, the silicon film actuator does not undergo any lithiation and does not function at all because of the lack of sufficient electrochemical driving force. That is to say, the output actuation strain is 0% for large loads exceeding a critical level. Fig. 2b shows the strain of actuation attained by the nanoscale flat-film actuator as a function of the applied pressure P. A salient feature of the plot is a jump in the strain of actuation from 300% for small loads to 0% for comparatively large loads. The jump is corresponding to the critical value of P beyond which the mechanical resistance becomes sufficiently large to counteract the driving force. By setting $\Delta G_{mech} = e\phi - \Delta G_{chem}$, the critical pressure marking the sharp transition in actuation strain is obtained as 5.61 GPa, 6.48 GPa, and 7.35 GPa for $P = 0.5$ V, 0.6 V, and 0.7 V, respectively. One notes that obtained critical pressure can also be interpreted as the maximum loading capacity of the actuator. It has been evident in Fig. 2b that the higher the input voltage, the larger the maximum load. It should be pointed out that the nanoscale flat-film actuator possesses extremely high actuation strain of 300% and extremely low driving voltage below 1 V.

The strain of actuation of the nanoscale flat-film actuator is either 300% or 0%, which is not tunable. Nevertheless, in applications from as small as nano-positioning to as large as coronary stenting, tunable actuation strain is favorable. In this regard, we next perform analysis of a nanowire silicon actuator as sketched in Fig. 1b, with lithium ions entering the nanowire through its lateral surface. To simulate load surrounding the nanowire actuator that to be expanded or stented, a uniform pressure P is applied to the lateral surface of the actuator (Fig. 1b). As mentioned above, the lithiation of silicon proceeds by the movement of a sharp reaction front separating the pristine silicon phase and the fully lithiated phase (Fig. 1b), which partitions the silicon nanowire into three regions in terms of the stress state: (a) the unlithiated core under hydrostatic pressure, (b) the atomically-thick reaction front subjected to circumferential compression, and (c) the fully lithiated shell undergoing tensile hoop stress [14,21]. Since the lithiation-induced elongation of the lithiated shell along the axial direction is constrained by the stiff silicon core, the nanowire is assumed to deform under plane-strain condition. The accuracy of the assumption has been verified by finite element simulations [20]. We derived the stress field in a lithiated silicon nanowire in our previous work [20]. To focus on the main ideas, here we only summarize the key results below. The radial, hoop, and axial stresses on the reaction front ($r = A$) are given by

$$\begin{cases} \sigma_r = \dfrac{2}{\sqrt{3}}\sigma_Y \log\left(\dfrac{A}{b}\right) - P \\ \sigma_\theta = -\sigma_Y + \dfrac{2}{\sqrt{3}}\sigma_Y \log\left(\dfrac{A}{b}\right) - P \\ \sigma_z = -\sigma_Y + \dfrac{2}{\sqrt{3}}\sigma_Y \log\left(\dfrac{A}{b}\right) - P \end{cases} \tag{8}$$

where A is the radius of the lithiation front and b the current radius of the nanowire. Therefore the mean stress on the reaction front is given by $\sigma_{\mathrm{m}}^{Li_{3.75}Si} = -\frac{2}{3}\sigma_Y + \frac{2}{\sqrt{3}}\sigma_Y \log\left(\frac{A}{b}\right) - P$. The stress field in the elastic silicon core can be solved as a plane-strain problem with $\varepsilon_z = 0$, it gives

$$\begin{cases} \sigma_r = \dfrac{2}{\sqrt{3}}\sigma_Y \log\left(\dfrac{A}{b}\right) - P \\ \sigma_\theta = \dfrac{2}{\sqrt{3}}\sigma_Y \log\left(\dfrac{A}{b}\right) - P \\ \sigma_z = \dfrac{4\nu}{\sqrt{3}}\sigma_Y \log\left(\dfrac{A}{b}\right) - 2P\nu \end{cases} \tag{9}$$

where ν denotes the Poisson's ratio of the pristine silicon. The mean stress in the unlithiated core is $\sigma_m^{Si} = \frac{4(1+\nu)}{3\sqrt{3}}\sigma_Y \log\left(\frac{A}{b}\right) - \frac{2(1+\nu)}{3}P$. Substituting $\sigma_{\mathrm{m}}^{Li_{3.75}Si}$ and σ_m^{Si} into Eq. (2) yields the expression of the mechanical resistance ΔG_{mech} of the nanowire silicon actuator,

$$\Delta G_{mech} = \frac{\Omega^{Si}}{3.75}\left[\frac{4(1+\nu) - 6\beta_{max}}{3\sqrt{3}}\sigma_Y \log\left(\frac{A}{b}\right) + \frac{2}{3}\sigma_Y\beta_{max} + \frac{3\beta_{max} - 2(1+\nu)}{3}P\right] \tag{10}$$

Fig. 3 a plots the evolution of ΔG_{mech}. The magnitude of ΔG_{mech} is shown as a function of the radius of reaction front A/b. Unlike the constant ΔG_{mech} in a flat-film actuator, it is found that the magnitude of ΔG_{mech} for the nanowire actuator gradually increases as A/b decreases, indicating that the mechanical resistance to drive load rises as the reaction front moves towards the center of the nanowire. The increasing resistance over time may become large enough to offset the driving force $e\phi - \Delta G_{chem}$, resulting in the halt of the lithiation reaction and thus stalling the actuator. Take a nanowire actuator which is connected to $\phi = 0.6$ eV and carries a load of $P = 5$ GPa (blue line in Fig. 3a) as an example. The driving force $e\phi - \Delta G_{chem} = 0.78$ eV, as highlighted by the

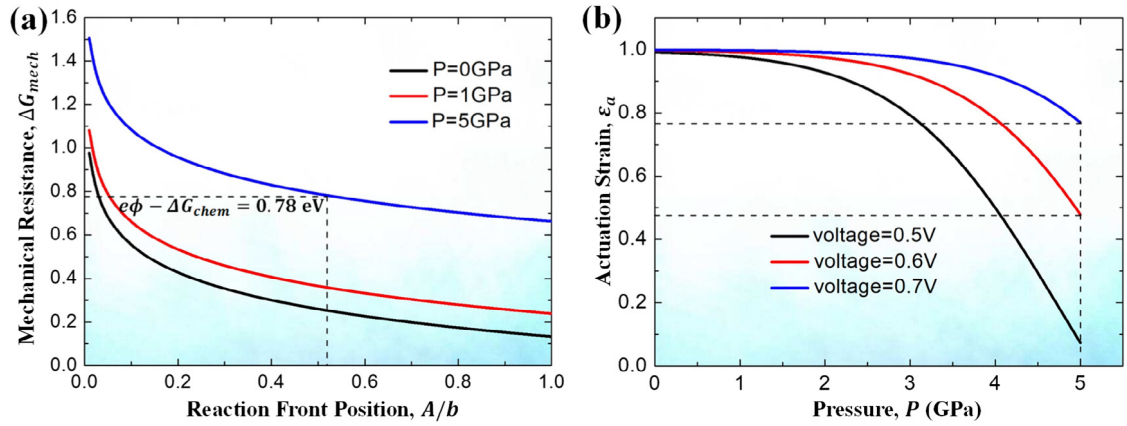

Fig. 3. (a) The mechanical resistance at different reaction front radii A/b. Note that the value of A/b decreases as the lithiation advances since the reaction front moves towards the center of the nanowire. (b) The output actuation strain with different applied voltages Φ and mechanical loads P. Given a load P, the output strain can be programmed by tuning the applied voltage Φ . (For interpretation of the references to color in this figure legend, the reader is referred to the web version of this article.)

horizontal dashed line in Fig. 3a. It is evident that the resistance ΔG_{mech} is below the driving force $e\phi - \Delta G_{chem}$ when $A/b > 0.52$, but surpass the driving force when $A/b < 0.52$. It implies that the nanowire actuator functions at the beginning but stalls eventually, ending up an unreacted silicon core electrochemically inaccessible characterized by $\tilde{A}/\tilde{b} = 0.52$, where $\tilde{A}$ denotes the final radius of the reaction front after the lithiation/actuation halts and $\tilde{b}$ the final outer radius of the nanowire. Furthermore, we set forth to investigate the effect of load on the performance of the actuator by varying P to 1 GPa and 0 GPa, respectively. The comparison between the cases reveals that a reduced load engenders a reduction in mechanical resistance ΔG_{chem}, giving rise to a smaller remaining silicon core after lithiation halts.

The strain of actuation of a nanowire actuator can be defined as $\varepsilon_a = \frac{\tilde{b}}{B} - 1$, where B is the initial radius of the nanowire actuator. Note that the final outer radius $\tilde{b}$ of the nanowire is related to B by $\tilde{b} = \sqrt{\beta_{max}\left(B^2 - \tilde{A}^2\right) + \tilde{A}^2}$, so that $\tilde{b}/B$ can be written as

$$\frac{\tilde{b}}{B} = \sqrt{\frac{\beta_{max}}{(\beta_{max} - 1)\left(\frac{\tilde{A}}{\tilde{b}}\right)^2 + 1}} \tag{11}$$

where $\beta_{max} = 4$ and the value of $\tilde{A}/\tilde{b}$ is determined by the intersection of the mechanical-resistance curve and the driving-force curve in Fig. 3a. Given an applied voltage Φ, Eq. (11) gives the strain of actuation ε_a. As shown in Fig. 3b, the actuation strain approaches 100% for small loads, namely, the theoretical limit corresponding to the complete lithiation of the entire silicon nanowire. An important feature of the nanowire actuator is the tunable actuation strain. In stark contrast to the nanoscale flat-film silicon actuator featuring a fixed output strain of 300%, the actuation strain of a nanowire silicon actuator decreases monotonically as the applied load P increases, endowing the nanowire actuator with tunable strains of actuation, which is particularly advantageous in applications such as nano-positioning. For instance, in Fig. 3b, a load of $P = 5$ GPa can be displaced with $\varepsilon_a = 48\%$ and 77% by setting the voltage to 0.6 V and 0.7 V, respectively. The results also indicate that nanowire actuator connected to a higher voltage can drive the mechanical load with a larger actuation strain. In summary, the nanowire silicon actuator not only possesses high actuation strain (up to 100%) and low driving voltage (below 1 V), but also features tunable actuation strain which is not attainable for the nanoscale flat-film actuator.

We report that nano-sized silicon under lithiation can be exploited as an electrochemically-driven actuator, by taking advantage of the significant lithiation-induced volume expansion. The theoretically-achievable strain of actuation is 300% for the thin-film actuator and 100% for the nanowire actuator, which are comparable to dielectric elastomers (such as VHB). More importantly, the driving voltage of the nano-sized silicon actuator is remarkably low, which is about 1 V, two orders of magnitude lower than piezoelectric ceramics/polymers and three orders of magnitude smaller than the dielectric elastomers. Fig. 4 demonstrates the comparison between lithiated silicon and other electroactive actuating materials in the space of driving voltage and actuation strain. The theoretical analysis performed in this work predicts that nanoscale silicon under lithiation exhibits the highest actuation strain and the lowest driving voltage. Additionally, owing to the high yielding stress of lithiated silicon, which is about 1.5 GPa, the silicon actuator has an output actuation stress beyond 1 GPa, outperforming existing actuating materials. The theoretically proposed nanoscale silicon actuators perform better than the macroscale actuator based on a LiFePO4/Si battery [8]. The difference can be attributed to the fracture-averting property of the nano-sized silicon and the strong mechanical constraints within a LiFePO4/Si full cell. However, we would like to point out that the working principle of the nano-actuators based on lithiation of silicon requires the contact between silicon and the lithium source, such that the setup of the practical silicon-based nano-actuators might be complex compared to other nano-positioning devices. We thus call for further experimental studies to verify and rationalize the predictions from the present theoretical study.

We conclude by a few remarks. In addition to the actuation strain and stress, actuation speed is also one of the key performance indicators for actuators. Herein, we estimate the actuation speed of silicon-based nano-actuators: The first lithiation of nano-sized silicon with a characteristic size of hundreds of nanometers usually takes about 100 s to complete [26]. As aforementioned, the flat-film actuator possesses an actuation strain of 300% and the nanowire actuator exhibits an output strain up to 100%. Accordingly, the average actuation speed, defined as the maximum actuation strain divided by the full lithiation time, is approximately 3% s^{-1} and less than 1% s^{-1} for the flat-film actuator and nanowire actuator, respectively.

The analysis in this work focuses on the first lithiation of silicon-based nano-actuators which is reaction-controlled. In contrast, the subsequent lithiation of post-lithiated silicon is diffusion-controlled [26]. Herein, we briefly discuss how the actuation performance of silicon nano-actuators in the second

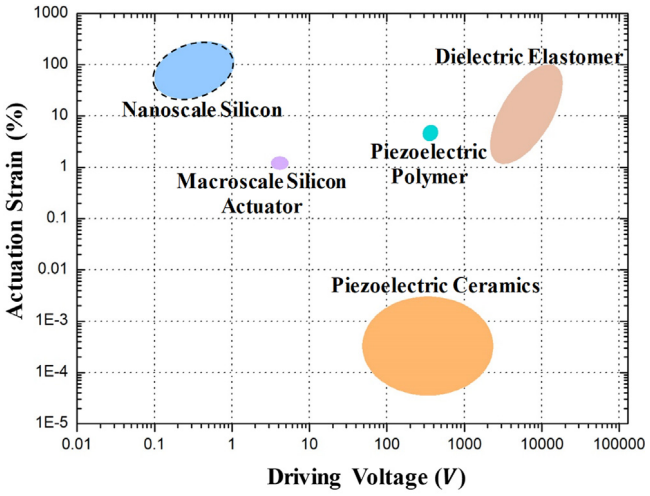

Fig. 4. Comparison between lithiated silicon and other actuator materials in terms of the driving voltage and the strain of actuation.
Source: Data are extracted from Refs. [8,22–25].

and subsequent cycles is affected by the diffusion-induced stress and the resulting overpotential. Bucci et al. showed that the diffusion-induced stress in silicon electrodes can generate an overpotential and thus modify the maximum capacity of the device [27]. The coupling of the overpotential and stress has been evaluated to be 62 mV/GPa for amorphous silicon in thin-film configurations [28]. The hydrostatic stress in the silicon actuators could reach several GPa (e.g., the hydrostatic stress near the reaction front in the thin-film actuator subject to P = 8 GPa is about 7.3 GPa), thus the overpotential due to diffusion-induced stress in silicon-based actuators (after the first cycle) is estimated to be hundreds of mV, on the same order of the overpotential in silicon nano-actuators in the first cycle (e.g., ∼700 mV for flat-film actuators under $P = 5$ GPa, as shown in Fig. 2a). To this end, the nano-actuator in the subsequent cycles functions for small loads since the stress-induced overpotential cannot counteract the electrochemical driving force, while the actuation halts for heavy loads because of excessive overpotential. The maximum actuation stress can be estimated as the stress which generates an overpotential of hundreds of mV and thus is on the order of several GPa. Moreover, as revealed by Bucci et al. the diffusion-induced overpotential affects the maximum volume change of the Si electrode [27], thereby rendering actuation strains between 0% and 300%, depending on the magnitude of the load and the configuration of the actuator.

Notably, cyclability is also pivotal to the success of actuators. It is reported that nano-sized silicon electrodes below a critical size (e.g. about 150 nm in diameter for crystalline silicon sphere and 300 nm in diameter for crystalline silicon nanowire) exhibit crack-averting property during the first cycle [29,30]. Amorphous silicon particles with a diameter of about 400 nm remain structurally intact for more than one single cycle [26]. Crystalline silicon nanowires with a diameter of 89 nm undergo ten charging/discharging cycles without apparent capacity fading induced by structural degradation [2]. To this end, it is concluded that silicon-based nano-actuators can function for several cycles. But the long-term cyclability of silicon-based nano-actuators might be limited because of the poor chemomechanical stability of silicon during repeated cycling.

It is well known that the pristine silicon, germanium, and tin all undergo two-phase lithiation, which features a sharp interface between the lithiated phase and the pristine phase [31–33]. In this study, we choose silicon as the actuator material only because values of all parameters (e.g., ΔG_{chem}) needed for the calculation are available in the literature, largely due to the fact that silicon has been widely investigated as the most promising anodes for Li-ion batteries. Since the first lithiation of silicon is similar to that of germanium and tin, the results of silicon-based actuators in terms of the actuation strain, stress, speed and cyclability also qualitatively apply to actuators based on germanium and tin.

In conclusion, we theoretically design nanoscale electrochemically-driven mechanical actuators based on the lithiation reaction of nano-sized silicon. The nano-actuators can drive a large mechanical load on the order of 1 GPa with a considerable actuation strain up to 300%, by taking advantage of the gigantic volume induced by the lithiation reaction. The driving voltage, which is below 1 V, is extremely low, compared to common actuator materials such as dielectric elastomer and piezoelectric ceramics which usually operate under voltage beyond 100 V. Moreover, given a mechanical load, the strain of actuation of the proposed nanowire silicon actuator is tunable, allowing for precise positioning of the load. The nanoscale silicon actuator holds promise in applications such as nano-positioners or nano-valve. Our findings provide rational guidance to the design of the more advanced actuating materials.

Declaration of competing interest

The authors declare that they have no known competing financial interests or personal relationships that could have appeared to influence the work reported in this paper.

Acknowledgments

Z. J. is grateful for the support of National Natural Science Foundation of China (Grant number: 11802269). Z. J. also acknowledges the financial support from the One-Hundred Talents Program of Zhejiang University.

References

[1] L.Y. Beaulieu, K.W. Eberman, R.L. Turner, L.J. Krause, J.R. Dahn, Colossal reversible volume changes in lithium alloys, Electrochem. Solid State Lett. 4 (9) (2001) A137–A140.
[2] C.K. Chan, H. Peng, G. Liu, K. McIlwrath, X.F. Zhang, R.A. Huggins, Y. Cui, High-performance lithium battery anodes using silicon nanowires, Nat. Nanotechnol. 3 (1) (2008) 31–35.
[3] Z. Lu, N. Liu, H.-W. Lee, J. Zhao, W. Li, Y. Li, Y. Cui, Nonfilling carbon coating of porous silicon micrometer-sized particles for high-performance lithium battery anodes, Acs Nano 9 (3) (2015) 2540–2547.
[4] Y. Jin, S. Li, A. Kushima, X. Zheng, Y. Sun, J. Xie, J. Sun, W. Xue, G. Zhou, J. Wu, F. Shi, R. Zhang, Z. Zhu, K. So, Y. Cui, J. Li, Self-healing SEI enables full-cell cycling of a silicon-majority anode with a coulombic efficiency exceeding 99.9%, Energy Environ. Sci. 10 (2) (2017) 580–592.
[5] Q. Xiao, M. Gu, H. Yang, B. Li, C. Zhang, Y. Liu, F. Liu, F. Dai, L. Yang, Z. Liu, X. Xiao, G. Liu, P. Zhao, S. Zhang, C. Wang, Y. Lu, M. Cai, Inward lithium-ion breathing of hierarchically porous silicon anodes, Nature Commun. 6 (2015).
[6] W. An, B. Gao, S. Mei, B. Xiang, J. Fu, L. Wang, Q. Zhang, P.K. Chu, K. Huo, Scalable synthesis of ant-nest-like bulk porous silicon for high-performance lithium-ion battery anodes, Nature Commun. 10 (2019).
[7] S. Choi, T.-W. Kwon, A. Coskun, J.W. Choi, Highly elastic binders integrating polyrotaxanes for silicon microparticle anodes in lithium ion batteries, Science 357 (6348) (2017) 279–283.
[8] J. Lang, B. Ding, T. Zhu, H. Su, H. Luo, L. Qi, K. Liu, K. Wang, N. Hussain, C. Zhao, X. Li, H. Gao, H. Wu, Cycling of a lithium-ion battery with a silicon anode drives large mechanical actuation, Adv. Mater. 28 (46) (2016) 10236–10243.
[9] M.-S. Noh, H. Lee, Y.G. Song, I. Jung, R. Ning, S.W. Paek, H.-C. Song, S.-H. Baek, C.-Y. Kang, S. Kim, Li alloy-based non-volatile actuators, Nano Energy 57 (2019) 653–659.
[10] N. Muralidharan, J. Afolabi, K. Share, M. Li, C.L. Pint, A fully transient mechanical energy harvester, Adv. Mater. Technol. 3 (8) (2018).

[11] S. Kim, S.J. Choi, K. Zhao, H. Yang, G. Gobbi, S. Zhang, J. Li, Electrochemically driven mechanical energy harvesting, Nature Commun. 7 (2016).
[12] T. Chen, H. Yang, J. Li, S. Zhang, Mechanics of electrochemically driven mechanical energy harvesting, Extreme Mech. Lett. 15 (2017) 78–82.
[13] X.H. Liu, J.W. Wang, S. Huang, F. Fan, X. Huang, Y. Liu, S. Krylyuk, J. Yoo, S.A. Dayeh, A.V. Davydov, S.X. Mao, S.T. Picraux, S. Zhang, J. Li, T. Zhu, J.Y. Huang, In situ atomic-scale imaging of electrochemical lithiation in silicon, Nature Nanotechnol. 7 (11) (2012) 749–756.
[14] H. Yang, F. Fan, W. Liang, X. Guo, T. Zhu, S. Zhang, A chemo-mechanical model of lithiation in silicon, J. Mech. Phys. Solids 70 (2014) 349–361.
[15] Z. Jia, T. Li, Intrinsic stress mitigation via elastic softening during two-step electrochemical lithiation of amorphous silicon, J. Mech. Phys. Solids 91 (2016) 278–290.
[16] B. Ding, H. Wu, Z. Xu, X. Li, H. Gao, Stress effects on lithiation in silicon, Nano Energy 38 (2017) 486–493.
[17] S. Zhang, Chemomechanical modeling of lithiation-induced failure in high-volume-change electrode materials for lithium ion batteries, Npj Comput. Mater. 3 (2017).
[18] M. Pharr, K. Zhao, X. Wang, Z. Suo, J.J. Vlassak, Kinetics of initial lithiation of crystalline silicon electrodes of lithium-ion batteries, Nano Lett. 12 (9) (2012) 5039–5047.
[19] K. Zhao, M. Pharr, Q. Wan, W.L. Wang, E. Kaxiras, J.J. Vlassak, Z. Suo, Concurrent reaction and plasticity during initial lithiation of crystalline silicon in lithium-ion batteries, J. Electrochem. Soc. 159 (3) (2012) A238–A243.
[20] Z. Jia, T. Li, Stress-modulated driving force for lithiation reaction in hollow nano-anodes, J. Power Sources 275 (2015) 866–876.
[21] S. Huang, F. Fan, J. Li, S. Zhang, T. Zhu, Stress generation during lithiation of high-capacity electrode particles in lithium ion batteries, Acta Mater. 61 (12) (2013) 4354–4364.
[22] S.H. Low, G.K. Lau, High actuation strain in silicone dielectric elastomer actuators with silver electrodes. 2011.
[23] R.K. Sahu, K. Patra, In evaluation of area strain response of dielectric elastomer actuator using image processing technique, Electroact. Polym. Actuators Devices (2014).
[24] G.W. Bohannan, V.H. Schmidt, R.J. Conant, J. Hallenberg, C. Nelson, A. Childs, C. Lukes, J. Ballensky, J. Wehri, B. Tikalsky, E. McKenzie, Piezoelectric Polymer Actuators in a Vibration Isolation Application Proceedings of SPIE, Vol. 3987, 2000, pp. 331–342.
[25] K. Wen, J. Qiu, H. Ji, K. Zhu, Fabrication of macro piezoceramic fiber composite actuators by cutting-filling method, J. Mater. Eng. 43 (2015) 72–76.
[26] M.T. McDowell, S.W. Lee, J.T. Harris, B.A. Korgel, C. Wang, W.D. Nix, Y. Cui, In situ TEM of two-phase lithiation of amorphous silicon nanospheres, Nano Lett. 13 (2) (2013) 758–764.
[27] G. Bucci, T. Swamy, S. Bishop, B.W. Sheldon, Y.-M. Chiang, W.C. Carter, The effect of stress on battery-electrode capacity, J. Electrochem. Soc. 164 (4) (2017) A645–A654.
[28] V.A. Sethuraman, M.J. Chon, M. Shimshak, V. Srinivasan, P.R. Guduru, In situ measurements of stress evolution in silicon thin films during electrochemical lithiation and delithiation, J. Power Sources 195 (15) (2010) 5062–5066.
[29] X.H. Liu, L. Zhong, S. Huang, S.X. Mao, T. Zhu, J.Y. Huang, Size-dependent fracture of silicon nanoparticles during lithiation, Acs Nano 6 (2) (2012) 1522–1531.
[30] S.W. Lee, M.T. McDowell, L.A. Berla, W.D. Nix, Y. Cui, Fracture of crystalline silicon nanopillars during electrochemical lithium insertion, Proc. Natl. Acad. Sci. USA 109 (11) (2012) 4080–4085.
[31] J.W. Wang, Y. He, F. Fan, X.H. Liu, S. Xia, Y. Liu, C.T. Harris, H. Li, J.Y. Huang, S.X. Mao, T. Zhu, Two-phase electrochemical lithiation in amorphous silicon, Nano Lett. 13 (2) (2013) 709–715.
[32] J. Wang, F. Fan, Y. Liu, K.L. Jungjohann, S.W. Lee, S.X. Mao, X. Liu, T. Zhu, Structural evolution and pulverization of tin nanoparticles during lithiation-delithiation cycling, J. Electrochem. Soc. 161 (11) (2014) F3019–F3024.
[33] W. Liang, H. Yang, F. Fan, Y. Liu, X.H. Liu, J.Y. Huang, T. Zhu, S. Zhang, Tough germanium nanoparticles under electrochemical cycling, Acs Nano 7 (4) (2013) 3427–3433.